EPSC 482: RESEARCH IN EARTH AND PLANETARY SCIENCE

Sensitivity analyses of sea level model outputs to ice history using the Travelling Time Window algorithm

April 27, 2022

Tomas Milla-Koch
260732843

INTRODUCTION

Understanding the past ice-loading history and associated isostatic deformation of the Earth's solid surface is essential to understanding the spatial and temporal evolution of global sea level over glacial timescales. Due to the viscoelasticity of the solid Earth's structure, solid Earth deformation in response to ice-sheet changes is sustained over hundreds of thousands of years. As a result, modelling sea-level change at a specific time requires the ice loading history leading up to that time, making simulations over glacial cycles computationally expensive.

Developed by graduate student Holly Han, the Travelling Time Window (TTW) algorithm is a tool that aims to tackle this challenge. Already implemented into a pseudo-spectral sea level model, the TTW algorithm was made to narrow down the periods and details of ice loading history necessary for pertinent sea level information used for research in geodynamics and paleoclimate. However, the precise details and memory of past ice loading changes that will affect the solid Earth are not yet constrained. Therefore, to test the validity of the TTW algorithm and its metrics, numerous sea level model runs were used to analyze the sensitivity of model results. The runs employed different Earth structure model parameters and different lengths and details of ice loading history with the aim to constrain time frames for which it is 'acceptable' to forget past ice loading history. Essentially, an expected outcome of the project is optimized parameters that characterize the length and details of ice loading history required for multiple glacial-cycle sea-level model simulations. The project's overarching aim was to contribute to extending the applicability of the sea-level model to ice age research problems.

TRAVELLING TIME WINDOW ALGORITHM

In order for the sea level model to run, it requires input ice history files that contain ice loading information at any given time step. From there, the pseudo-spectral sea level model will implement all the necessary physics to calculate global bedrock elevation evolution. Sea level is then calculated by a simple relationship:

$$SL(\theta, \psi, t_j) = G(\theta, \psi, t_j) - R(\theta, \psi, t_j) \tag{1}$$

where **R** is the bedrock elevation, **G** is the reference geoid, θ is the colatitude, ψ is the east-longitude, and $\mathbf{t_j}$ is the time (Mitrovica & Milne, 2003; Kendall et al., 2005; Dalca et al., 2013). Therefore, the TTW controls the amount of physics that is being incorporated into the model over the entire run with ice history files that are generated by an ice sheet model (Pollard & DeConto, 2012).

The TTW algorithm separates the model memory of ice loading history into 2 sections; an external TTW and a cluster of internal time windows (TWs), known as dt1, dt2, etc. (Figure 1). The external TTW is the full extent of time over which the sea level model simulations will incorporate ice history at the smallest time step. In other words, the TTW will 'march' forward, hence 'travelling' over every time step defined in the model for the length of the TTW (Figure 1). Internal TWs differ in that an internal TW shorter than the length of the simulation will not necessarily forget ice files as a TTW shorter than the simulation length would. The internal TWs represent the entire TTW being broken up into separate time frames over which ice file detail is ignored over a certain defined period of time (Figure 1). For example, if the TTW is the same length as the entire simulation but the fist internal TW covers a shorter period of time, then sea level changes as a result of ice-loading changes within the first internal TW will be accounted for as the internal TW marches forward. In this case, ice files are not being forgotten because they were already incorporated within the first internal TW, depite it

marching forward in time.

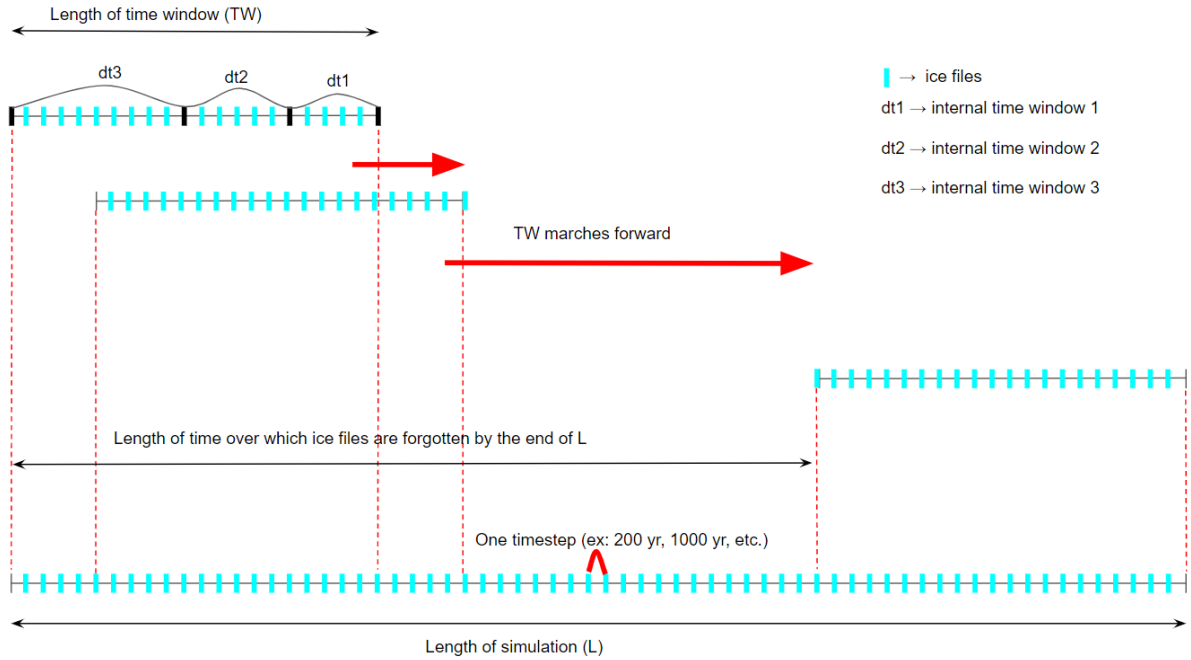

Figure 1: Conceptual model of the TTW algorithm and the iterative process over which it is implemented into the sea level model.

METHODS

This research project was effectively divided into three steps; attempting to observe glacial isostatic adjustment (GIA) features of a solid Earth response to glacial unloading, analysing bedrock changes when varying internal TTW distributions, and analysing varying full TTW lengths and their effect on bedrock elevation changes over glacial cycles. An expected outcome was that of an optimized TTW length for sea level simulations over glacial cycles. The word optimize here, implies that there will always be error in the sea level calculations performed by the model when you incorporate the TTW algorithm. This is true because, at any given TTW less than the simulation length, the model is effectively ignoring some ice history. However, as the solid Earth responds viscoelastically to unloading of ice, there would be some ice files that are more important in terms of sea level change than others. For

example, we would expect that the majority of isostatic rebound be confined to the period of time where elastic response and viscoelastic response reresents the greatest signal of solid Earth change (i.e. directly after unloading of ice). Therefore, the question is whether or not there are TTW lengths, internal and external, that can achieve similar results to runs with the same ice configurations but, with no TTWs incorporated?

0.1 Solid Earth Response

For simplicity, the same conditions were used regarding time of unloading as well as ice configuration. The simulation itself was a simple one, a water planet where there is one massive ice sheet placed on the geographic south pole (Figure 2). As the center of the ice sheet would have the greatest center of mass, the bedrock topography (also fixed) was set to have a downgrading slope where the weight of the ice would be greatest and there would be an opposing continent in the northern latitudes (Figure 3). As for the ice unloading, the ice was unloaded entirely at once, in other words, the ice sheet melted completely from one time step to the next. To leave enough room to visualize the solid Earth response, the ice sheet was unloaded at 120 ka and the solid Earth response was allowed to run until 0 ka. The sea level model took in pre-generated ice files at every time step, which were designed to be every 10 ky. This allowed changes in bedrock elevation to be seen every 10 ky after the initial unloading episode at 120 ka.

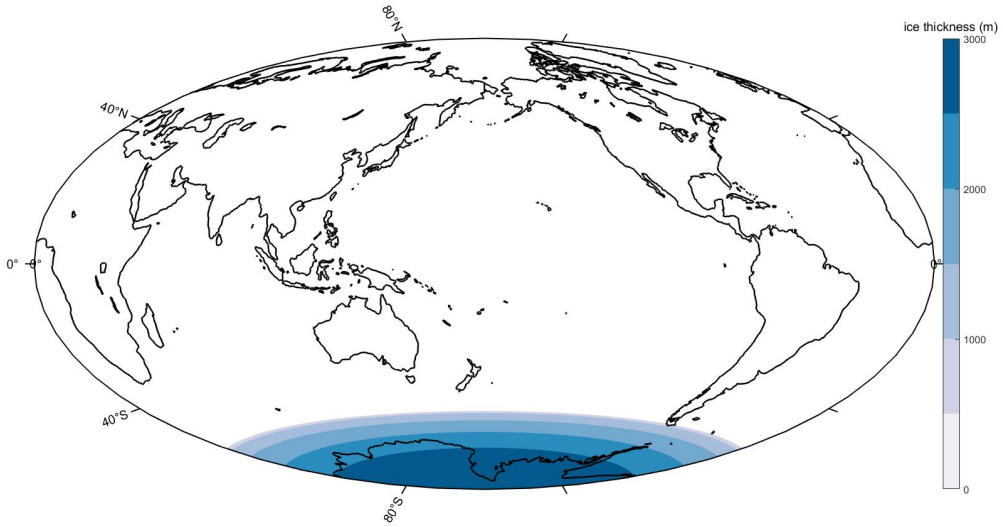

Figure 2: Projected ice sheet used for model runs.

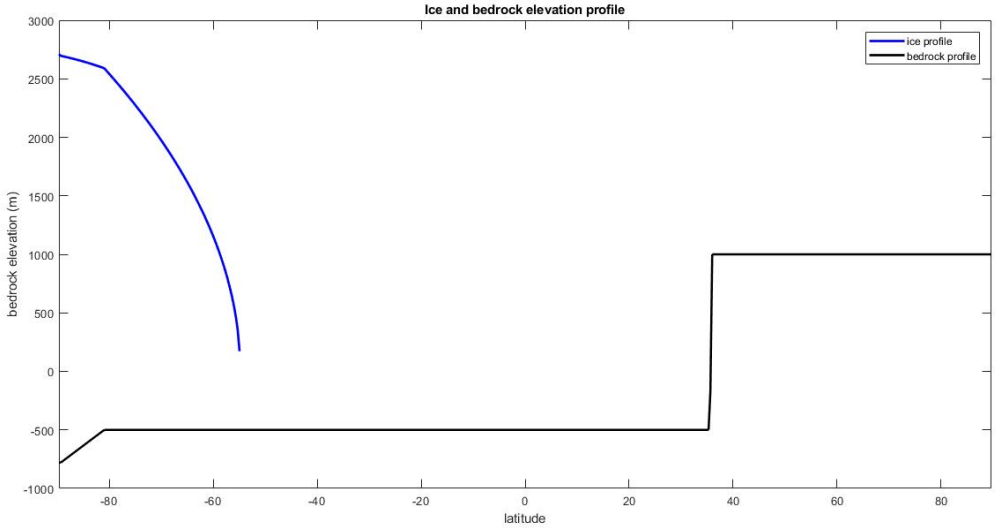

Figure 3: Global cross-section of the ice and bedrock topography profiles, equally distributed for all longitudinal cross-sections. Note that the fixed bedrock topography profile has a down graded slope where the center of loading is and a makeshift continent rising in higher northern latitudes. This is meant to simulate a bedrock topography that subsides under the larger weight of ice at the center of loading and the spreading of mantle material to compensate.

In addition, six different preliminary Earth reference models (PREM) were used to test the sensitivities of the solid Earth response following the unloading in the simulations. All

PREM models had varying structural viscosity components for the upper and lower mantles. In summary, six different models runs were performed with six different PREM models.

0.2 Internal TTW distribution tests

To test the internal TTW distribution, a more realistic ice configuration and unloading scenario was used. The ice configuration chosen was that at the last glacial maximum (LGM); Ice 5G (Figure 4a). The simulation length was equalt to 122 ky. where the Ice 5G configuration was then melted over 22 ky in order to mimic the deglaciation from the LGM to present. The ice configuration at the model's 100 ka (Figure 4b) was then unchanged over 100 ky until 0ka. This was done to observe the isolated solid Earth response to the changing of ice in the first 22 ky of the model run. To test the sea level model output sensitivity to internal TTW distributions, times of 10, 20, 40, 60, and 80 ky were chosen for dt2 (second internal time window). In other words, dt1 was equal to 112, 102, 82, 62, and 42 ky respectively for each model run (Figure 1;5). This meant that the number of ice files read into the sea level code, relative to the time the model has run, is dependent on whether or not dt1 has been reached or not. Once dt1 is reached, at each following time step, the code will ignore that ice loading history until, at the end of the simulation, the amount of ice files that were ignored would correspond to the time period covered by dt2 (Figure 5). Finally, a control run where bedrock elevation changes were calculated at each 1 ky time step was used for sensitivity tests (Figure 5). In addition, the PREM model used for all runs was the VM2 model (Peltier, 1996).

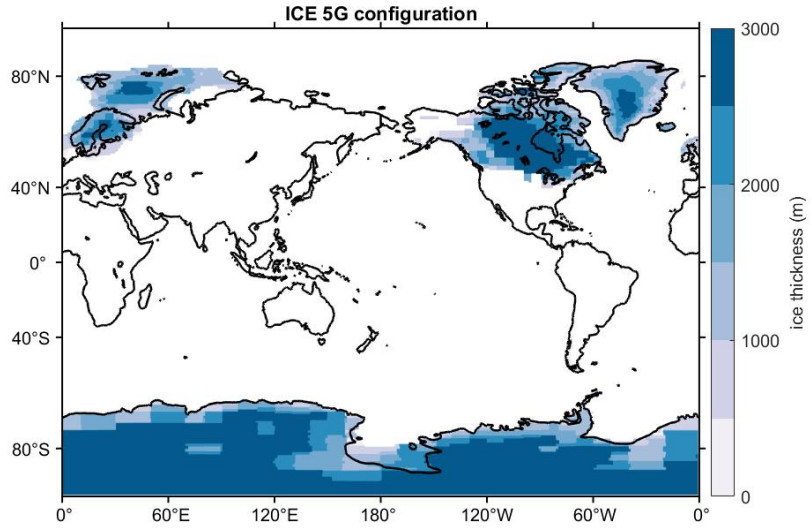

(a)

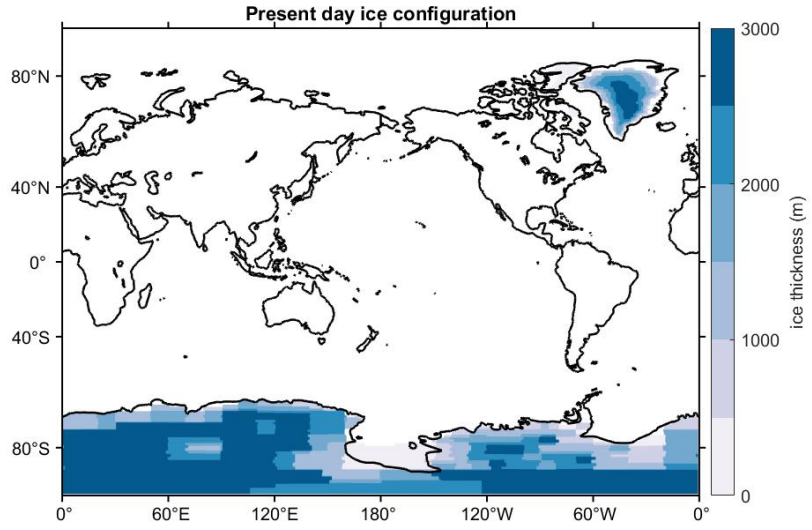

(b)

Figure 4: Endpoint ice configurations: **(a)** Ice 5G configuration for beginning of simulation (122 ka), and **(b)** Present day ice configuration for end of deglaciation phase in the simulation (100 ka).

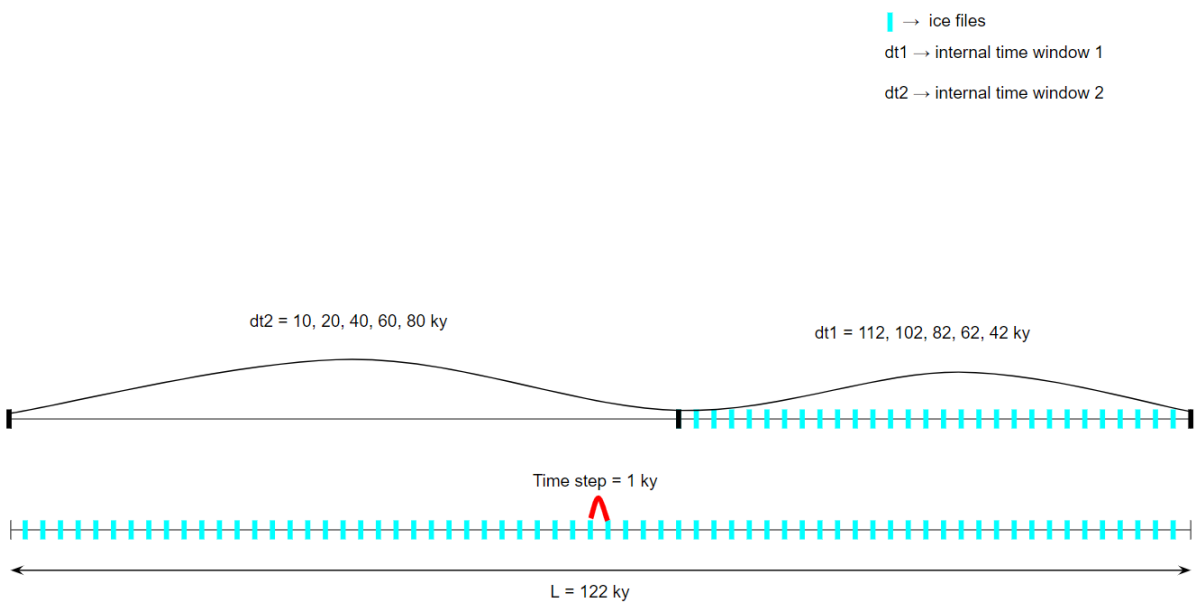

Figure 5: TTW algorithm schematic for the internal TTW distribution sensitivity tests.

0.3 Full TTW tests

Testing for full TTWs implemented into the model were done using the exact same unloading scenario as for the internal TTW distribution tests. The control run was also the same and used for comparison. The TTW lengths used were 10, 20, 40, 60 ky. The shorter lengths were used in an attempt to observe what the model output errors are when we forget ice history in the first 22 ky of deglaciation while the longer lengths would represent TTWs that account for these ice-loading changes. The PREM model used for all runs was the VM2 model (Peltier, 1996).

RESULTS

As mentioned in the methodology, the first step in the analysis was observing the outputs from the sea level model for a one time step ice unloading scenario (i.e.130ky long simulation

with entirety of ice being unloaded at 120 ka). What was expected is for the bedrock profile to undergo its most drastic deformation directly following the unloading of ice. This effect is the elastic solid Earth response to glacial unloading. What follows is the solid Earth's more drawn out viscous plus elastic (viscoelastic) response to glacial unloading. At the moment in time where the elastic responses and viscous responses are contributing equally to solid Earth rebound is when the response is expected to be greatest (i.e. Maxwell time) (Peltier, 1974). In addition, we expect the solid Earth response to be the most pronounced where there was enough overlying ice mass in the loading phase to create a substantial depression in the solid Earth as low as the lower mantle (Peltier, 1974). These responses are expected to last as long as >100 ky as the lower mantle will continue to redistribute material long after the initial unloading sequence, regardless of the upper mantle's movement prior (Peltier, 1974).

The greatest response from the solid Earth as a result of glacial unloading is indeed seen where the ice actually was prior to unloading time at 120 ka (Figure 5). Seen also is the depression of the global bedrock profile in the equatorial regions following the unloading time. This is evidence of ocean siphoning. Where there is a glacial mass to the scale of an ice sheet, the mass will distort the Earth's gravitational field so that the Earth's sea water will be attracted to the Earth's ice sheets as they gain mass. However, with the unloading of ice, the gravitational field will be distorted once more and melt water as a result of melting ice sheets will be siphoned to the equatorial bulges with enough mass to physically suppress the bedrock profile (Figure 6).

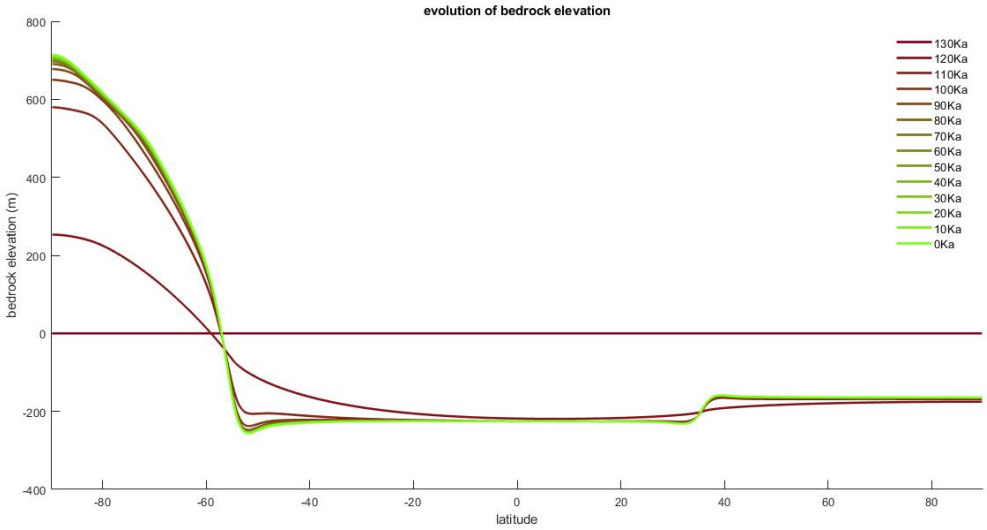

Figure 6: Global bedrock elevation evolution for a simulation of 130 ky with entirety of ice being unloaded at 120 ka. Note the latitude horizontal axis corresponding to **Figure 3**, effectively showing that the largest responses are indeed where ice previously sat on top of the bedrock profile.

We also see that the mass of the ice sheet is large enough that in order for mass to be compensated once unloaded, mantle material from as far as the northern latitudes where there was a continent (Figure 3;6) flows to lower latitudes. However, we also see that the responses are are not uniform in time (Figure 6). That is to say that the rate of changes of bedrock elevation changes between each time step (i.e. 10 ky) are not consistent. However, again, this is to be expected as the majority of the solid Earth response happens relatively close after the unloading time. These rates of change, however, are pertinent for confining the length of a TTW. In theory, the length of any TTW should cover the majority of bedrock changes following unloading in order to minimize sea level change error over glacial timescales. As for model runs, outputs of the runs are also dependent of what kind of PREM model is used. In this case, 6 different PREM models were used to attempt to track solid Earth responses for differently structured Earths. Depending on the layered viscosity structure of the modelled Earth, responses may be faster or slower in time with different magnitudes relative to the unloading event. Forgetting the simulation, this combination of different viscosities at different

layers of the Earth (i.e. upper and lower mantle) will also affect the solid Earth response over the past glacial timescales due to the constant loading and unloading of the solid Earth that occurs over a glacial cycle, creating a multi-normal mode response (Peltier, 1974).

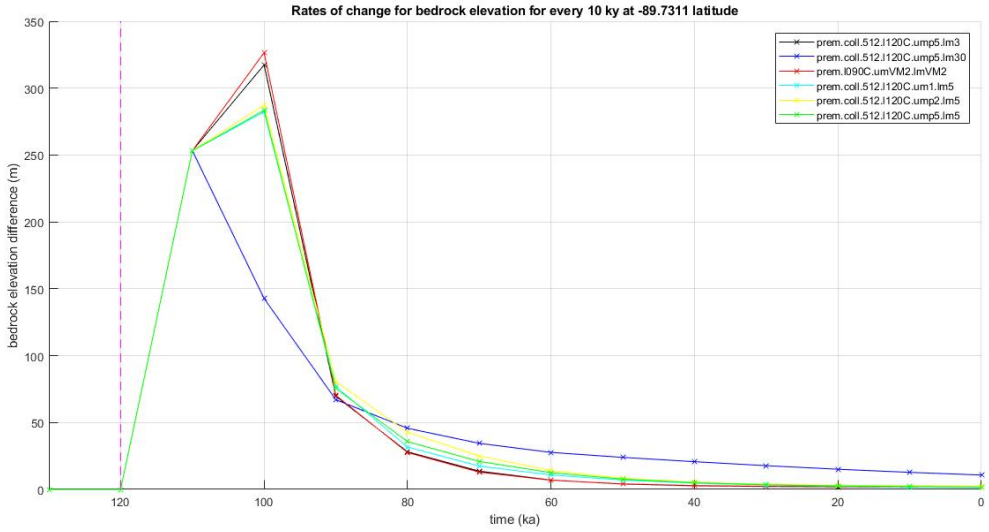

(a) Center of ice sheet.

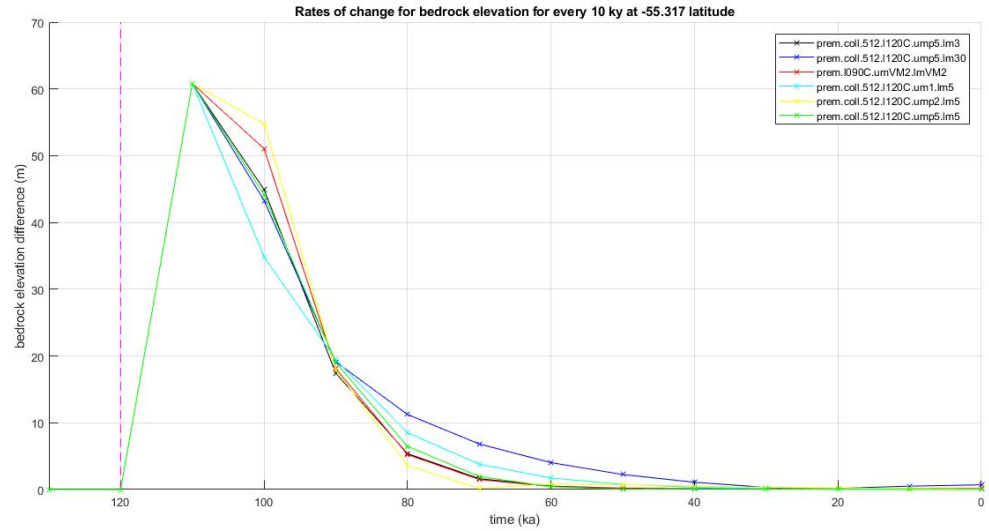

(b) Edge of ice sheet.

Figure 7: Rates of change between every time step (every 10 ky) of bedrock elevations following ice unloading at the latitude corresponding to the (a) center of the ice load and the (b) edge of the ice load. The output bedrock elevation changes result from six simulations each, using six different PREM models. In black, a PREM model with a lithospheric thickness of 120 km, an upper mantle viscosity of 5 x 10^{20} Pa·s, and a lower mantle viscosity of 3 x 10^{21} Pa·s. In dark blue, a PREM model with a lithospheric thickness of 120 km, an upper mantle viscosity of 5 x 10^{20} Pa·s, and a lower mantle viscosity of 3 x 10^{22} Pa·s. In red, a PREM model with a lithospheric thickness of 120 km, the viscosity structure details can be found in Peltier (1996). In light blue, a PREM model with a lithospheric thickness of 120 km, an upper mantle viscosity of 1 x 10^{21} Pa·s, and a lower mantle viscosity of 5 x 10^{21} Pa·s. In yellow, a PREM model with a lithospheric thickness of 120 km, an upper mantle viscosity of 2 x 10^{20} Pa·s, and a lower mantle viscosity of 5 x 10^{21} Pa·s. In green, a PREM model with a lithospheric thickness of 120 km, an upper mantle viscosity of 5 x 10^{20} Pa·s, and a lower mantle viscosity of 5 x 10^{21} Pa·s. Note that the solid Earth relaxation time is shorter for lower viscosity models. In this scenario, ice is also being unloaded completely at 120 ka, where unloading time is marked by a dashed magenta line.

As previously mentioned, knowing which amount of ice history that can be forgotten requires constraining the length of the TTW. Ideally, this window length is characterized by the length of time that corresponds to the greatest change in bedrock elevation (i.e. sea level change). Thus, an approximate TTW window length could be comparable to that of the mean e-folding time for all runs ~ 40-50 ky as demonstrated by the largest curves of **Figure 6**. However, with respect to these rate of change curves, we still see that there is residual change happening until the end of the simulation, implying that there is still important GIA effects taking place after the majority of the solid Earth response has happened (Figure 6). Thus, assuming the that sea level calculations will be fairly accurate with basing the TTW length on the e-folding time would be inaccurate due to the extended solid Earth response. Therefore, sensitivity tests are necessary for constraining the optimal TTW length. As per described in the **Methods** section, the internal time window distributions were first tested, followed by the varying lengths of full TTWs.

Modifying the internal TTW distribution does not mean that ice history will be forgotten once the first internal TW is reached (Figure 1;5) but, that the ice history incorporated into the length of the first internal TW will be ignored for sea level change calculations as soon as the first internal TW length is reached in the simulation. Therefore, we would expect that the longer the first internal TW, the more closely the sea level calculations would resemble a control run's where no internal TW was employed in the model and bedrock elevation changes were calculated at every time step. The results of the tests performed are displayed in **Figure 7**.

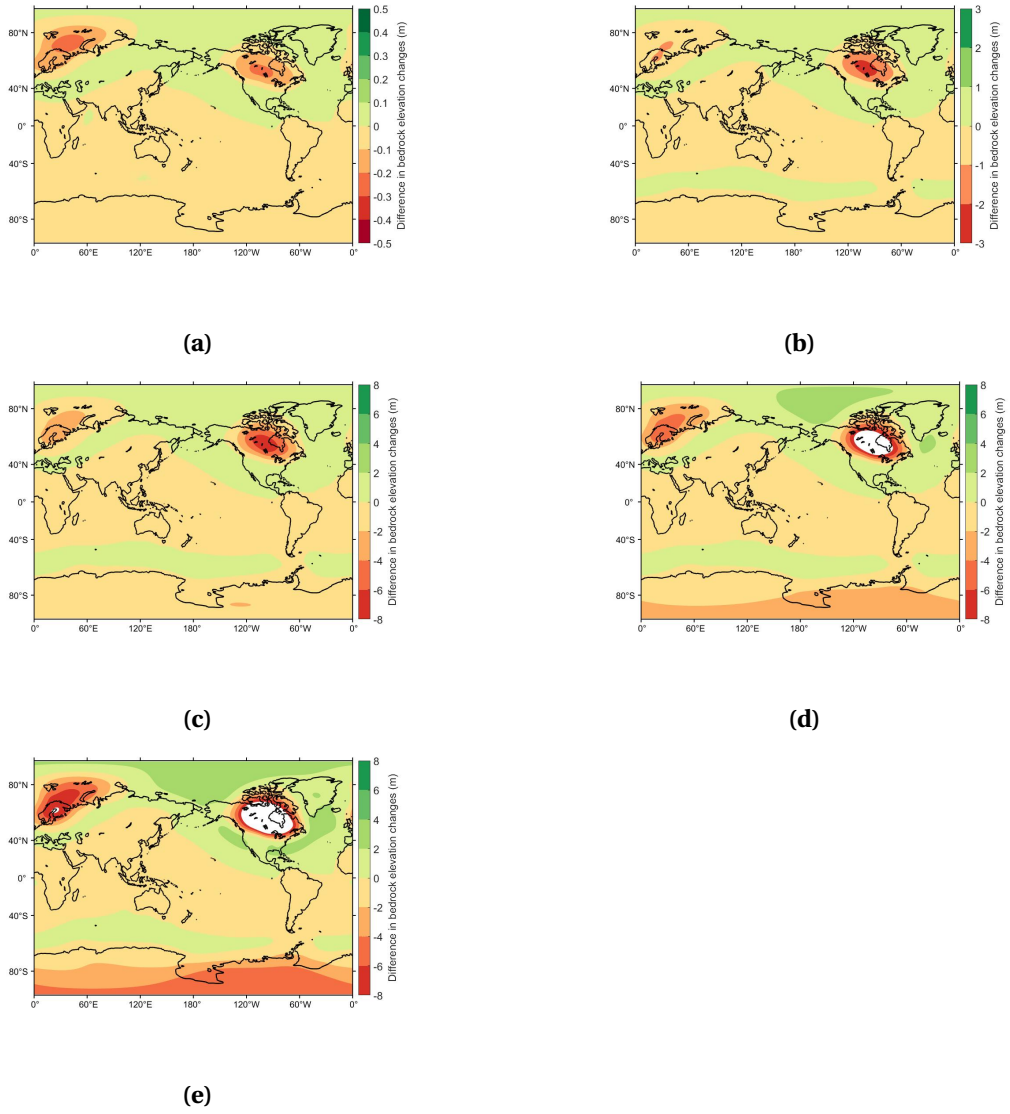

Figure 8: Miller projections of differences between control and test runs for beginning to end of simulation bedrock elevation changes (i.e. Δ**R(122-0 ka)** between control and test runs). All test runs have their TWs equaling to the length of the simulation where the only component altered is that of the internal TW distribution (i.e. dt1 length). Here, (a) dt1=112 ky, (b) dt1=102 ky, (c) dt1=82 ky, (d) dt1=62 ky, and (e) dt1=42 ky.

As expected, the longer the first internal TW (dt1), the more closely the resulting total simulation bedrock elevation change resembles the control run (Figure 7). Thus, an important question is to what degree the results resemble the control run. If we take differences between control run and model run results for three locations, we find that degrees of difference between the test and control runs differently pronounced. The three locations in question

include one of maximum bedrock elevation difference between the model runs (i.e. Hudson's bay), one from a peripheral bulge observable in Figure (i.e. the Denmark strait), and finally one from the equatorial region that experiences very little difference in all model runs (Figure 8).

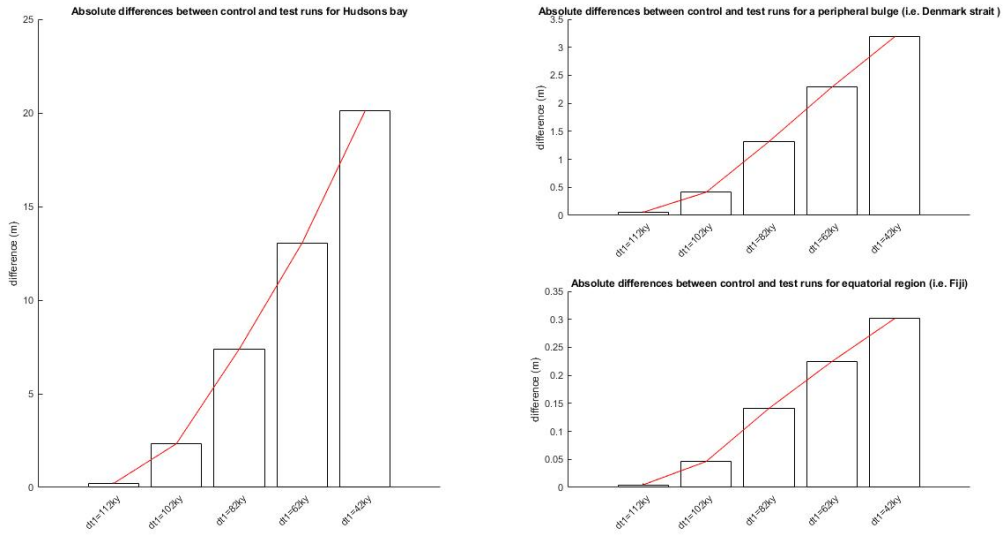

Figure 9: Differences between control and test runs for beginning to end of simulation bedrock elevation changes (i.e. Δ**R(122-0 ka)** between control and test runs) for different regions of interest; Hudson's bay, a peripheral bulge of the Laurentian ice sheet (Denmark strait) and an island in the equatorial zone (Fiji).

We find that, for the simulations, Hudson's bay experiences the largest difference between control runs and internal TW runs when dt1 is equal to 42 ky (an absolute difference of 22 m). While 22 m is a substantial error in projected sea level change, the error is not so large when we consider the total bedrock elevation change from the beginning to end of the control run. A maximum absolute difference of 22 m between a test run where dt1=42 ky and the control run over 122 ky of simulation time to a total bedrock elevation change of 1300 m over 122 ky yields a ~2% maximum error in sea level change. In addition, if we look at the root mean square error (RMSE) of the internal TW test runs in relation to the control run, we see that RMSE values are only as high as ~2.5 m for a dt1 of 42 ky, which implies a mean erro of ~0.2% (Figure 9). We also notice that the RMSE distribution appears 'linear' and only begins for

each test run once each respective dt1 length is reached (Figure 9). A simple test could then be performed to validate whether this distribution makes sense or not (see **Appendix 1**).

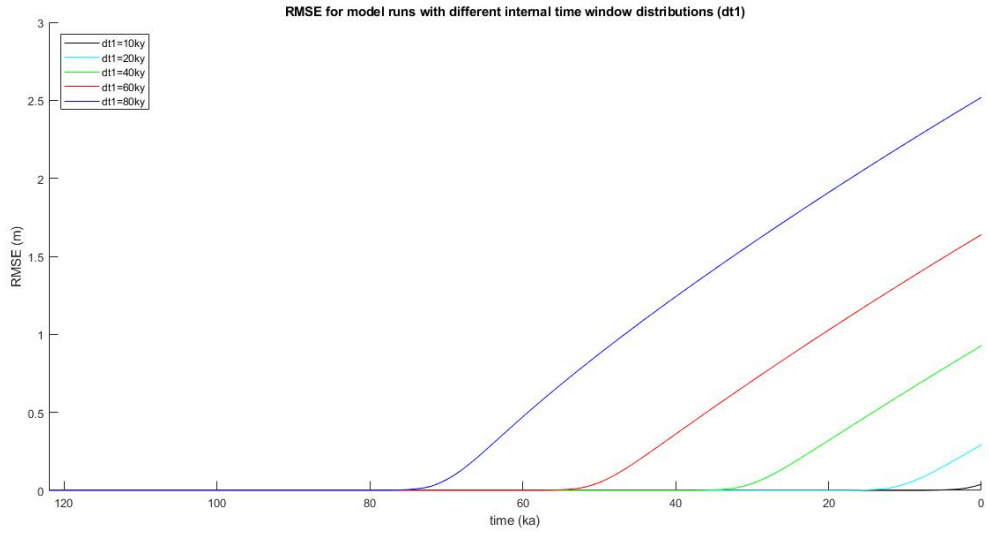

Figure 10: RMSE for test runs where only the dt1 lengths are changing between test runs.

How can this relationship be explained? A possible reason is that when testing for different dt1 lengths, each dt1 length accounts for the first 22 ky the simulation, consequently the total time of ice loading changes. Therefore, there is no dynamic solid Earth unloading not being accounted for in the simulations. The differences are therefore resulting from residual differences between the control and test runs that could be of prolonged multi-normal mode responses from the lower mantle that occurs long after ice unloading would have stopped (Peltier, 1974).

However, if the overarching goal is to reduce the computational time of sea level model runs over glacial timescales, then full TTW lengths must be tested and compared to the control run as opposed to simply changing dt1 lengths. For these test runs, for one, we would expect larger errors as ice loading history is actively being forgotten after every time step once the TTW has grown fully (Figure 1). Therefore, the shorter the TTW, the larger the difference we would expect from differences between the control run and test runs. These results are

explored in **Figure 11**.

In summary, differences between control runs to test runs do indeed increase as the TTW length grows shorter (Figure 11). This presents essential information on how the sea level model is run. Ice loading details, regardless of whether they be during a more dynamic time frame (i.e. during glaciation or deglaciation) or not, will affect the sea level calculation of the proceeding time step because forward sea level change calculations between time steps requires the previous time step's ice details for the calculation to even be performed. By that logic, in an implemented TTW run, the ice details over a solid Earth response time of any given time step would be always be different the control run results because the proceeding time step ice loading information would be forgotten as soon as the TTW is fully grown. In comparison, the control run, having every ice file inputted into the code at every respective time step, would output a different total sea level change. We can analyze these differences by taking the RMSE over the entire simulation length for different TTW lengths.

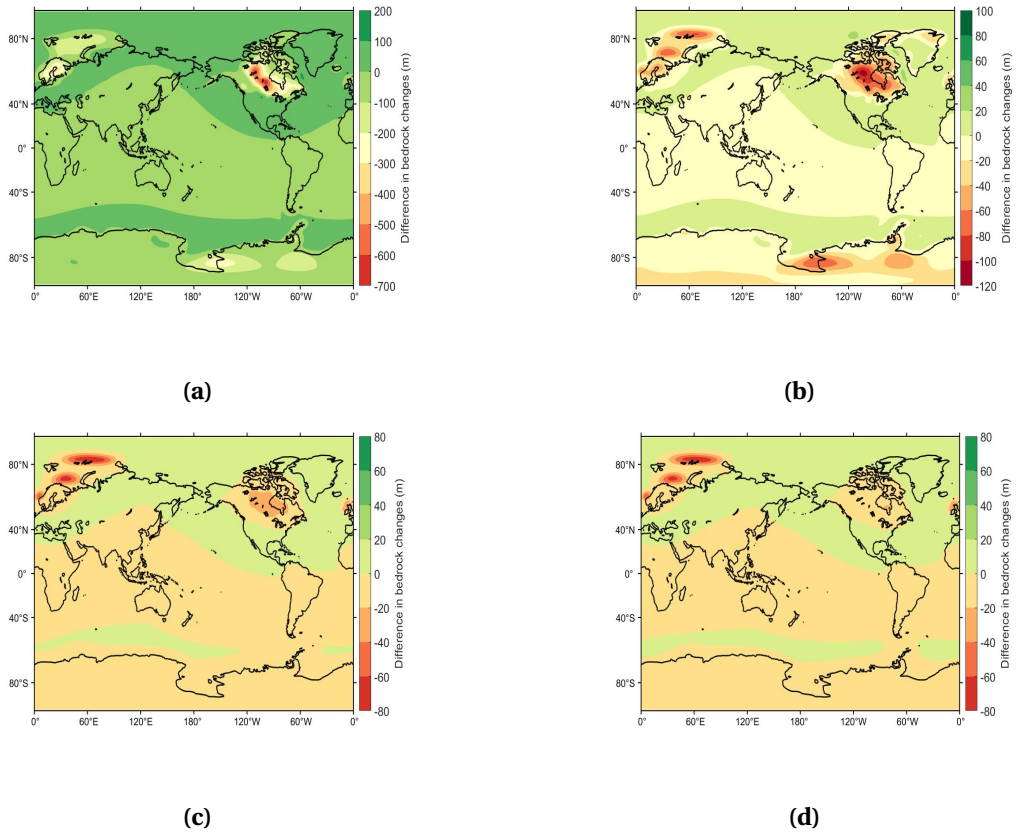

Figure 11: Miller projections of differences between control and test runs for beginning to end of simulation bedrock elevation changes (i.e. Δ**R(122-0 ka)** between control and test runs). Here, all test runs have different TTW legnths where (a) dt1=10 ky, (b) dt1=20 ky, (c) TTW=40 ky, and (d) TTW=60 ky. Note the scale bar changes between differences.

We find that the RMSE is represented by cyclical pulses and drops in error magnitude that are much larger than the previous test of the varying internal TW distribution (Figure 11). However, the shape of the RMSE distribution is also quite different from the RMSE error of the internal TW distribution test runs (Figure 11). A possible explanation is that every TTW length tested will forget ice history pertaining to the dynamic deglaciation phase (the first 22 ky of the simulation). This could be why we see a pulse of RMSE as soon as ice history is being forgotten (i.e. as soon as any given TTW is fully grown) (Figure 11). The period of the cyclic error appears equal to the length of the TTW. However, what causes the down gradient in RMSE? One explanation could be that once the SL change calculations start to read in ice

files that are not part of the deglaciation phase, then error will be lowered as ice history is not changing at all. This change will be present even if the TTW still accounst for dynamic ice loading changes within the ice files because the SL calculation is only taking into account for the time step previous to the current one for sea level calculations. However, after ~.212 of the TTW length from the peak of the RMSE rise, the error will rise again, most likely due to the embedded error from the first rise in RMSE. That being said, the previous theories are speculative and further exploration of these results is pertinent to understanding the RMSE distribution. The timing for this re rise in RMSE error, however, is only seen for test runs with TTW lengths of 10 and 20 ky. Curiously, test runs with TTW lengths of 40 and 60 ky experience a much more gradual fall in RMSE before it rises again (Figure 11). Perhaps, this is due to these test runs' TTWs covering the dynamic deglaciation phase in the first 22 ky of the simulation?

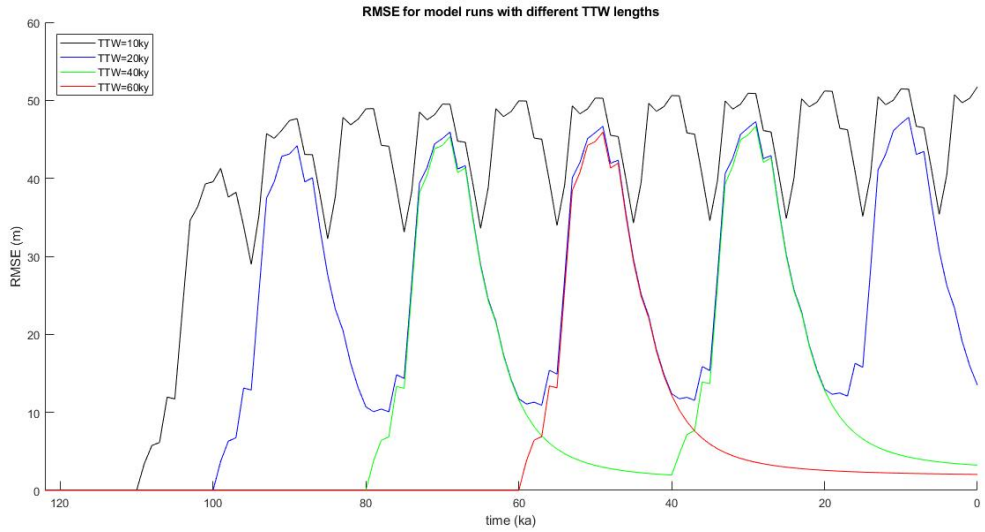

Figure 12: RMSE for the different test runs.

Thus, it can be concluded that runs using the TTW algorithm will have large associated error in beginning to end of simulation sea level calculations. These errors are an order magnitude greater than the error produced when we only modify the internal TW distribution of a TTW that is equal to the length of the entire simulation length (50% maximum error as

opposed to 2% maximum error) (see **Appendix 2**). While future work is needed to tell for certain whether or not models should include the TTW algorithm if they wish to accurately calculate sea level changes on glacial time scales, there is almost certain to be associated error due to the way sea level models are inherently set up. As previously mentioned, sea level calculations are calculated forward in time by calling on the ice history from the previous time step. If we consider a more realistic simulation where ice is constantly dynamically unloading and loading the solid Earth (i.e. deglaciation and glaciation over multiple glacial cycles), ice history from the previous time step will always incorporate dynamic history that would cause high RMSE values if ignored (Figure 12). The culprit for the inaccurate calculation of sea level is thus the time step over which details of ice history are incorporated into the sea level model. The hybrid ice sheet model, developed by (Pollard & DeConto, 2012), has been able to generate ice history down to 1000 year time steps where it can be further interpolated down to 200 years (Pollard et al., 2018). This is a time step that is now used in standard sea level model forward runs, both coupled to the ice sheet model and not (Pollard et al., 2018). While this is an incredible feat, it would change bedrock elevation height changes even for the simple simulations run for these analyses. This would simply be due to the fact that the previous time step ice history would alter the one forward in time so that bedrock elevation calculations would be different over 1000 year time steps as opposed to 200 year time steps.

CONCLUSION

Sea level calculations over a single glacial cycle are non-trivial in nature, let alone several glacial cycles. Detailed ice history is needed to accurately calculate these sea level changes so that they are able to be compared to observational sea level records. For detailed calculations, ice history files are needed to be incorporated into the sea level model at every time step where the range can be as short as 200 years per time step (Pollard et al., 2018). This amount of detail makes sea level model runs computationally expensive. The TTW algorithm's aim is to

reduce the computational power necessary to run these sea level models over multiple glacial cycle timescales, while still performing 'accurate' forward sea level changes. When we speak of sea level changes, the calculation is dependent on bedrock elevation changes (Kendall et al., 2005). Thus the solid Earth response will dominate global mean sea level signals over these time scales. However, isostatic equilibrium is rarely, if ever, reached after the unloading of ice sheets due to the prolongued GIA response from the upper and lower mantle. This makes it so there is no absolute length of the TTW that will accout for all important solid Earth response following an unloading event. therefore, there will always be associated error. These errors will be high if TTW lengths are short and forget ice history that is part of large dynamic ice mass changes (deglaciation or glaciation). These errors will be reduced if the TTW lengths account for said dynamic ice mass changes and will be even further reduced if only the internal TTW distribution is being changed relative to the length of the simulation. In order, however, for this algorithm to merit being steadily utilized in active cryospheric research, more sensitivity tests are needed. The simulations in this project were all uncoupled to a hybrid ice sheet model (Pollard % DeConto, 2012). Therefore, future studies should aim to incorporate large coupled runs as these runs require the most computational power, especially if these runs are occurs over glacial cycle time scales and at time steps of 200 years. Studies should also explore a more full extent of solid Earth responses using different PREM models or even 3D Earth structure models to observe a full range of possible solid Earth deformations. Solid Earth responses may vary in places where underlying viscosity is very low, for example, as is observed under the western Antarctic ice sheet.

APPENDIX

1 VERIFICATION FOR THE DISTRIBUTION SHAPE FOR RMSE FOR INTERNAL TW DISTRIBUTION TESTS

Figure 10 shows an RMSE plot where the distribution appears linear in shape. This is hypothesized to be because there are no dynamic ice loading changes on the solid Earth being ignored by the sea level model. A simple test was done to see why the shape resembles what it does. The bedrock elevation changes were taken from the beginning of the simulation (122 ka) to the end of each run's respective dt1 length (see **Methods** for lengths). The logic was that if for the duration of the dt1 length for each respective run calculates bedrock elevation changes the same way that the control run would, the differences between the runs' values should be zero until the control calculates changes beyond the time step where ice history is beginning to be ignored. The differences indeed show that bedrock change values between any test run and the control run do not change until the 2nd to 3rd time step after dt1 is reached. In other words, the results only begin to diverge in the period of 2-3 ky after dt1 is reached, and the change is very small, hence why we see a gradual increase in RMSE overtime (Figure 13).

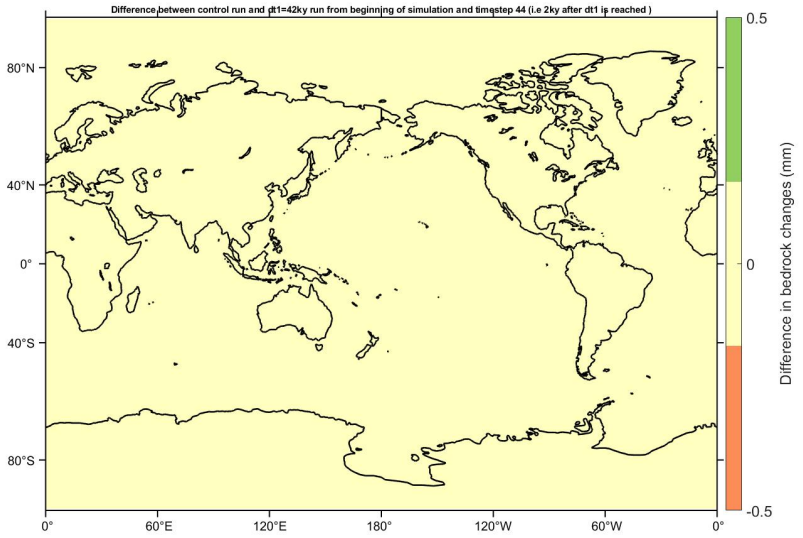

(a)

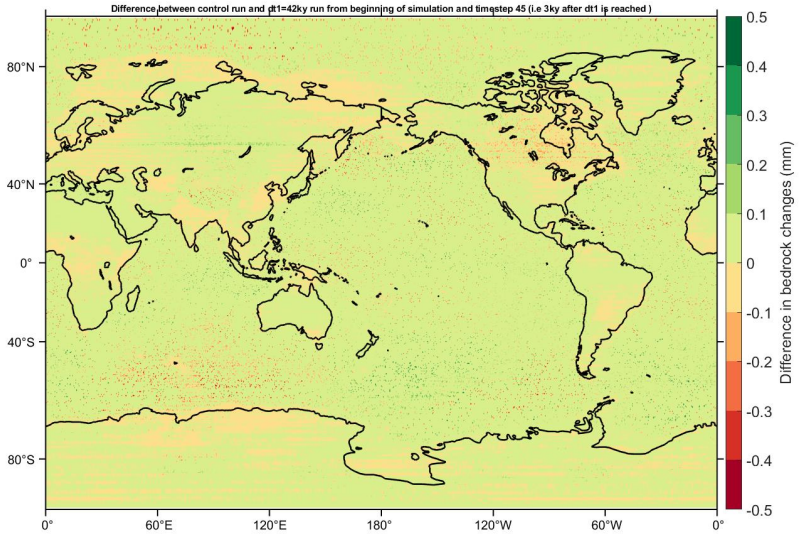

(b)

Figure 13: Difference between control run and run where dt1=42 ky from beginning of simulation to timestep **(a)** 44 (i.e. 2 years after dt1 is reached) and timestep **(b)** 45 (i.e. 3 years after dt1 is reached).

2 FULL TTW TEST DIFFERENCES FOR SET LOCATIONS

For comparison, differences between the control run and the varying TTW length test runs, more specifically their bedrock elevation changes, were taken and plotted for the same specific GIA effect related regions as for the internal TTW distribution tests. The locations were: an area of large glacial isostatic rebound after deglaciation (i.e. Hudson's bay), a peripheral bulge to the Laurentian ice sheet (i.e. the Denmark strait), and a region in the equator (i.e. Fiji) (Figure 14). Here, we see, as discussed before, that the larger the length of TTW, the lower the difference (Figure 14). We also see that the largest magnitudes of difference are for Hudson's bay, which was overlain by the Laurentian ice sheet at the LGM (Pollard et al., 2018). The differences are lower in magnitude when they are taken for the peripheral bulge, and even lower for the equator (Figure 14).

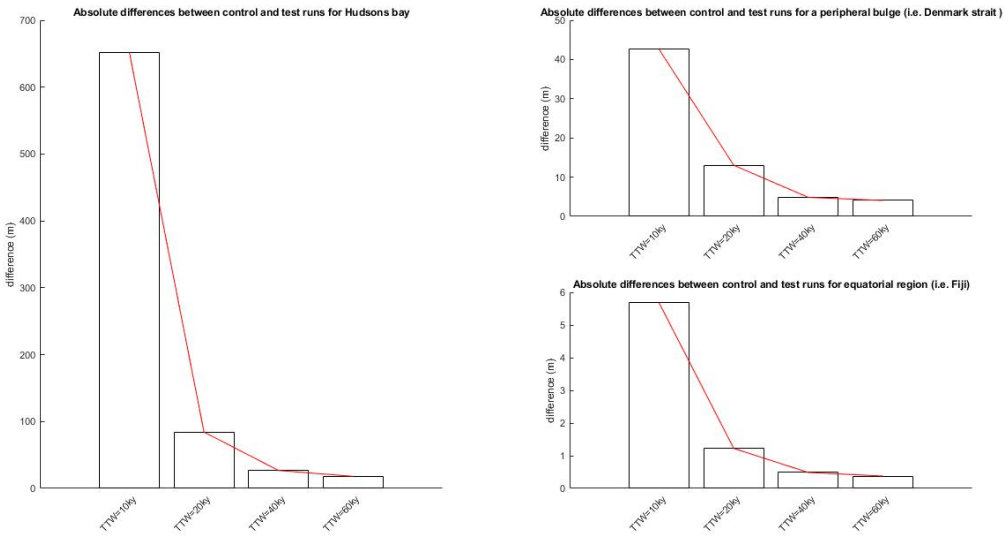

Figure 14: Beginning to end of simulation bedrock elevation change differences between control and test runs with varying TTW lengths. Note that the locations chosen are the same as per **Figure 9**

REFERENCES

Dalca, A.V., Ferrier, K.L., Mitrovica, J.X., Perron, J.T., Milne, G.A. & Creveling, J.R. On postglacial sea level—III. Incorporating sediment redistribution, Geophysical Journal International, Volume 194, Issue 1, Pages 45-60 (2013)

Kendall, R.A, Mitrovica, J.X. Milne, G.A. On post-glacial sea level: II. Numerical formulation and comparative results on spherically symmetric models, Geophys. J. Int., 161, 679-706 (2005)

Mitrovica, J.X. & Milne, G.A. On post-glacial sea level: I. General theory, Geophys. J. Int., 154, 253-267 (2003)

Peltier, W.R. The impulse response of a Maxwell Earth, *Rev. Geophys. Space Phys.*, 12, 649 (1974)

Peltier, W. R. Mantle viscosity and ice-age ice-sheet topography, Science, 273, 1359–1364 (1996)

Pollard, D. & DeConto, R. Description of a hybrid ice sheet-shelf model, and application to Antarctica. Geosci. Model Dev . 5, 1273–1295 (2012)

Pollard, D., Gomez, N., DeConto, R. M., & Han, H. K. Estimating Modern Elevations of Pliocene Shorelines Using a Coupled Ice Sheet-Earth-Sea Level Model. Journal of Geophysical Research: Earth Surface, 123(9), 2279-2291 (2018)